

Quantum Monte Carlo calculation of entanglement Rényi entropies for generic quantum systems

Stephan Humeniuk^{1,2} and Tommaso Roscilde¹¹Laboratoire de Physique, CNRS UMR 5672, Ecole Normale Supérieure de Lyon, Université de Lyon, 46 Allée d'Italie, Lyon, F-69364, France²Institut de Ciències Fotòniques i Òptiques, Avenida C. F. Gauss, numero 3, 08860 Castelldefels, Spain

(Received 30 March 2012; revised manuscript received 16 November 2012; published 12 December 2012)

We present a general scheme for the calculation of the Rényi entropy of a subsystem in quantum many-body models that can be efficiently simulated via quantum Monte Carlo. When the simulation is performed at very low temperature, the above approach delivers the entanglement Rényi entropy of the subsystem, and it allows us to explore the crossover to the thermal Rényi entropy as the temperature is increased. We implement this scheme explicitly within the stochastic series expansion as well as within path-integral Monte Carlo, and apply it to quantum spin and quantum rotor models. In the case of quantum spins, we show that relevant models in two dimensions with reduced symmetry (XX model or hard-core bosons, transverse-field Ising model at the quantum critical point) exhibit an area law for the scaling of the entanglement entropy.

DOI: [10.1103/PhysRevB.86.235116](https://doi.org/10.1103/PhysRevB.86.235116)

PACS number(s): 03.65.Ud, 02.70.Ss, 74.40.Kb

I. INTRODUCTION

Entanglement represents the unique correlation property of quantum states, and as such it can play a fundamental role in our understanding of quantum many-body phases from the point of view of nonlocal correlations. The most striking manifestation of entanglement in a quantum state $|\psi\rangle$ is represented by the mixed nature of the reduced density matrix ρ_A describing a subsystem A of a quantum many-body system, and defined as the partial trace of the total density matrix $\rho = |\psi\rangle\langle\psi|$ on the complement B , $\rho_A = \text{Tr}_B \rho$. The mixedness of ρ_A can be captured by any entropy estimator, the most common being the von Neumann entropy $S_A^{(\text{vN})} = -\text{Tr} \rho_A \ln \rho_A$, but one can equivalently use its generalization, the Rényi entropy¹

$$S_A^{(\alpha)} = -\frac{\ln[\text{Tr}(\rho_A^\alpha)]}{1-\alpha}, \quad (1)$$

which reduces to the von Neumann entropy in the limit $\alpha \rightarrow 1$. The calculation of entanglement entropies in quantum many-body states appears as a formidable task, as it seems to imply the necessity to reconstruct the reduced density matrix of a subsystem A ; this generally represents a hard problem unless A contains very few degrees of freedom. In fact this task can be performed efficiently only in a few cases, including noninteracting bosons and fermions on a lattice.² For these models, considering fully connected A regions (e.g., hypercubic ones) the scaling of the entanglement entropy with the linear size l_A of the region can be calculated analytically in the asymptotic limit $l_A \rightarrow \infty$. Analytical and numerical calculations show that most models obey a so-called area law $S_A^{(\alpha)} \sim l_A^{D-1}$ in D dimensions, except for critical models in $D = 1$ and free fermions with a $(D-1)$ -dimensional Fermi surface, in which case the area law is corrected by a multiplicative logarithmic term.³ Much less is known about models of interacting particles. Indeed their reduced density matrix can be in principle reconstructed efficiently via density-matrix renormalization-group (DMRG) and tensor-network algorithms in one-dimensional lattice systems. Yet, when extended to higher dimensions, these algorithms do not guarantee in general to reproduce the whole entanglement content of the wave function. It is also worth mentioning

that the calculation of the Rényi entropy for $\alpha = 2$ has been implemented for $SU(2)$ -invariant lattice spin models via a projector Monte Carlo technique in Ref. 4.

Here we propose a different technique to calculate the Rényi entropy of a subsystem, valid for *arbitrary* quantum many-body models which admit an efficient quantum Monte Carlo (QMC) solution of their equilibrium statistical properties. This includes models with a finite as well as an infinite Hilbert space. The basic idea is to perform the QMC simulation in an extended ensemble for α replicas of the system, treating the topology of the $(D+1)$ -dimensional configurations generated by QMC as a dynamical variable. We argue that this approach substantially improves on all existing schemes for the QMC estimate of the Rényi entropy. We demonstrate it for the calculation of the $\alpha = 2$ Rényi entropy both at (physically) zero and finite temperature, for two-dimensional $S = 1/2$ quantum spin models with low symmetry, as well as for the $O(2)$ quantum rotor model in $D = 1$.

The paper is structured as follows. Section II describes how the proposed approach applies to generic QMC schemes at finite temperature; Sec. III describes the implementation of this approach for one-dimensional lattice models (XX model and quantum rotor model), while Sec. IV discusses applications to two-dimensional quantum spin models, including the Heisenberg, XX , XY model and the transverse-field Ising (TFI) model at the quantum critical point. The two appendixes provide a detailed comparison with previously proposed methods, and a discussion of our results concerning the subleading terms in the scaling of the entanglement entropy for two-dimensional quantum spin systems.

II. QUANTUM MONTE CARLO ESTIMATOR OF THE RÉNYI ENTROPY

A. Rényi entropies as partition function ratios

Reference 5 has shown that, thanks to its trace structure, the Rényi entropy at finite temperature can be cast in the form of the logarithm of the ratio of partition functions,

$$S^\alpha = \frac{\ln R_A^{(\alpha)}}{1-\alpha}, \quad R_A^{(\alpha)} = \frac{\mathcal{Z}_A^{(\alpha)}}{\mathcal{Z}^\alpha}. \quad (2)$$

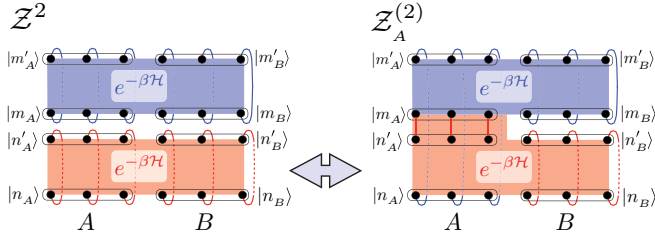


FIG. 1. (Color online) Transition from the \mathcal{Z}^2 to the $\mathcal{Z}_A^{(2)}$ sector by redefinition of the topology of the simulation box in the additional dimension. The blue/red regions and lines are associated with the action of the imaginary-time propagator $e^{-\beta\mathcal{H}}$. Solid lines link states which are connected by a propagation step.

Here $\mathcal{Z}^\alpha = [\text{Tr}(e^{-\beta\mathcal{H}})]^\alpha$ is the ordinary partition function for α replicas of the system, while $\mathcal{Z}_A^{(\alpha)}$ is a modified partition function for replicas which are “glued” together in the region A . This is best seen in the simplest case $\alpha = 2$, for which

$$\mathcal{Z}_A^{(2)} = \sum_{\substack{n_A, m_A \\ n_B, m_B}} \langle n_A n_B | e^{-\beta\mathcal{H}} | m_A n_B \rangle \langle m_A m_B | e^{-\beta\mathcal{H}} | n_A m_B \rangle. \quad (3)$$

Here $|n_A n_B\rangle$ is an arbitrary basis of states which are factorized between the A and B regions. Regarding $e^{-\beta\mathcal{H}}$ as the imaginary-time propagator, Eq. (3) describes a cyclic propagation for a time 2β of the A -region state, and two independent cyclic propagations for a time β of the B -region state, as sketched in Fig. 1. On the other hand \mathcal{Z}^2 describes two independent propagations for a time β . The statistical mechanics formulation of the Rényi entropy has been remarkably exploited in Ref. 5 for the calculation of the entanglement entropies for conformal field theories (CFTs); more recently Refs. 6–8 have implemented a quantum Monte Carlo calculation of both \mathcal{Z} and $\mathcal{Z}_A^{(\alpha)}$ separately via direct thermodynamic integration of the energy curve $E(\beta')$ over the interval $[0, \beta]$ to obtain the finite-temperature Rényi entropy $S_A^{(\alpha)}(\beta)$. This technique, while being very general, appears to be technically limited to finite temperatures,^{6,7} given that as $T \rightarrow 0$, the Rényi entropy is extracted as the difference between two diverging integrals, giving rise to an uncontrolled error (see Appendix A). Moreover, the integration approach implies that the system has a finite-dimensional Hilbert space, and therefore it is limited in practice to lattice models with discrete local degrees of freedom.

In the following we propose an alternative QMC approach which cures the above limitations, allowing us to systematically calculate the Rényi entropy of a subsystem with a *single* simulation at the temperature of interest, performed within an extended ensemble, for any model to which finite-temperature Monte Carlo methods can be applied, including models with an infinite-dimensional Hilbert space.

B. Extended-ensemble estimator

The central idea of our approach is that the ratio of two partition functions can be generally estimated with Monte Carlo by performing a simulation in an ensemble which is the union of the two, $\mathcal{Z}^2 \cup \mathcal{Z}_A^{(2)}$. Whichever quantum Monte Carlo approach is used for the estimation of the equilibrium

statistical properties of the Hamiltonian \mathcal{H} , it should allow us to write $\mathcal{Z}_A^{(2)}$ in the form

$$\mathcal{Z}_A^{(2)} = \sum_{\mathcal{C}} w_A(\mathcal{C}), \quad (4)$$

where $\mathcal{C} = (n_A, n_B; m_A, m_B; \mathcal{P})$ is a QMC configuration, in which the state $|n_A\rangle$ is propagated to $|m_A\rangle$ and then back to itself in the region A , while the states $|n_B\rangle$ and $|m_B\rangle$ are propagated onto themselves independently, and the propagation scheme is represented by \mathcal{P} : \mathcal{P} is generally a path in the computational basis $|\psi(\tau)\rangle = |\psi_A(\tau)\rangle|\psi_B(\tau)\rangle$ parametrized by the (continuous) imaginary time $\tau \in [0, \beta]$ as in path-integral Monte Carlo (PIMC),⁹ or by the propagation step index $\tau = p$, associated with a string of bond operators, as in stochastic series expansion (SSE).¹⁰ Within the above notation, $\mathcal{Z}^2 = \mathcal{Z}_{A=\emptyset}^{(2)}$. w_A is the statistical weight of a configuration; the Hamiltonian \mathcal{H} lends itself to an efficient QMC simulation if $w_A \geq 0$ for all configurations, and if the weights w_A can be calculated efficiently.

Our method consists in constructing a simulation which moves dynamically between the \mathcal{Z}^2 ensemble and the $\mathcal{Z}_A^{(2)}$ while respecting the detailed balance condition. The move from one ensemble to another can be performed with Metropolis probability

$$P(\mathcal{Z}^2 \rightarrow \mathcal{Z}_A^{(2)}) = \min[1, w_A(\mathcal{C})/w_{A=\emptyset}(\mathcal{C})] \quad (5)$$

and vice versa for the reverse move. The partition function ratio $R_A^{(2)}$ is then simply estimated as

$$R_A^{(2)} = \langle N_A / N_{A=\emptyset} \rangle_{\text{MC}}, \quad (6)$$

where N_A is the number of MC steps in the ensemble with a given region A , and $\langle \dots \rangle_{\text{MC}}$ is the Monte Carlo average. A straightforward generalization of the above formulas is possible for $\alpha > 2$. We would like to point out that an analogous extended-ensemble QMC scheme is the one defining the QMC estimator for observables which are off-diagonal in the computational basis.¹¹

In practice, for a simulation of discrete degrees of freedom on a lattice—e.g., quantum spins, lattice gases—with conserved quantities (total magnetization, particle number, etc.) the weights $w_A(\mathcal{C})$ and $w_{A=\emptyset}(\mathcal{C})$ cannot in general be simultaneously nonvanishing unless the condition $|n_A\rangle = |m_A\rangle$ is satisfied, in which case the transition in the propagation topology (Fig. 1) is microcanonical, namely $w_A(\mathcal{C}) = w_{A=\emptyset}(\mathcal{C})$. In the case of quantum spin systems or lattice gases without conserved quantities, or of continuous lattice variables—e.g., quantum rotors—of particles in continuous space, the “rewiring” of world lines demanded by the transition between the ensembles can be in principle always performed, although it will have an acceptance rate which is low if the configurations $|n_A\rangle$ and $|m_A\rangle$ are very different.¹² Assuming to use a PIMC scheme in which the imaginary time is discretized in steps $\Delta\tau$, and indicating with \mathcal{H}_{OD} the part of the Hamiltonian which is off-diagonal in the computational basis, one has that the ratio $w_A(\mathcal{C})/w_{A=\emptyset}(\mathcal{C})$ takes the expression

$$\frac{\langle n'_A n'_B | e^{-\Delta\tau\mathcal{H}_{\text{OD}}} | m_A n_B \rangle \langle m'_A m'_B | e^{-\Delta\tau\mathcal{H}_{\text{OD}}} | n_A m_B \rangle}{\langle n'_A n'_B | e^{-\Delta\tau\mathcal{H}_{\text{OD}}} | n_A n_B \rangle \langle m'_A m'_B | e^{-\Delta\tau\mathcal{H}_{\text{OD}}} | m_A m_B \rangle}. \quad (7)$$

As indicated in Fig. 1, the primed configurations are connected to the unprimed ones by a single propagation step.

The above scheme provides an efficient estimate of $R_A^{(\alpha)}$, and therefore of $S_A^{(\alpha)}$, by performing a single simulation at the temperature of interest. When the temperature is chosen to be so low as to remove thermal effects on a finite-size simulation box, one can gain access to the entanglement Rényi entropy.

III. RESULTS FOR ONE-DIMENSIONAL MODELS

Unless otherwise specified, in the following we will show simulation results for the general case of an XYZ Hamiltonian in a field

$$\mathcal{H} = J \sum_{\langle ij \rangle} (S_i^x S_j^x + \Delta_y S_i^y S_j^y + \Delta_z S_i^z S_j^z) - H \sum_i S_i^z, \quad (8)$$

where S_i^α are $S = 1/2$ spin operators, $J > 0$, and $\langle ij \rangle$ indicates a pair of nearest neighbors on a D -dimensional hypercubic lattice. A validation of our approach comes from the comparison with exact results in $D = 1$, which are available, e.g., for the case of the XX model ($\Delta_y = 1$, $\Delta_z = 0$); such a model admits a mapping onto a system of free fermions,¹³ whose entanglement properties can be calculated from the knowledge of two-point correlations.² Figure 2(a) shows the data for a $L = 64$ chain with periodic boundary conditions, simulated with the SSE algorithm; very good agreement is found between the exact results and QMC results at an inverse temperature $\beta J = 200$.

In principle the whole $S_A^{(2)}$ curve as a function of l_A can be obtained by performing simulations in the joint $\mathcal{Z}^2 \cup \mathcal{Z}_A^{(2)}$ ensemble; in practice, the transition rate between the two ensembles is strongly suppressed when the size of A grows, given that the condition $|n_A\rangle = |m_A\rangle$ is increasingly hard to satisfy. This aspect reflects the fact that the ratio $R_A^{(2)}$ estimated in the simulation decreases exponentially with $S_A^{(2)}$, $R_A^{(2)} = \exp(-S_A^{(2)})$. In the $D = 1$ case in question, in which⁵

$$S_A^{(\alpha)} \approx (\bar{c}/6)(1 + 1/\alpha) \ln l_A, \quad (9)$$

we obtain that $R_A^{(2)} \approx l_A^{-\bar{c}/4}$, where \bar{c} is the central charge of the related CFT. If an area law holds, one has an even more serious

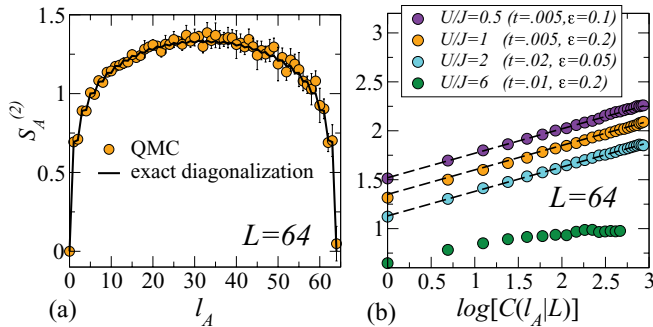


FIG. 2. (Color online) (a) Entanglement entropy of the one-dimensional (1D) XX chain; the solid line corresponds to exact diagonalization. (b) Entanglement entropy of the 1D $O(2)$ quantum rotor model. Here $L = 64$, $t = k_B T/J$, and $\epsilon = \Delta \tau U$; increments $\Delta l = 1$ are used; the dashed lines correspond to fits to the CFT prediction $(1/4)\ln[C(l_A|L)] + s_1$.

decrease $R_A^{(2)} \approx \exp(-\bar{c} l_A^{D-1})$. The events that the simulation has to count become increasingly rare, so that the simulation length should naively scale as $(R_A^{(2)})^{-1}$.

To cure this problem we use the *increment trick* from Ref. 4, by formally rewriting $R_A^{(2)}$ as

$$R_A^{(2)} = \prod_{i=0}^{N-1} R_{A_i, A_{i+1}}^{(2)}, \quad R_{A_i, A_{i+1}}^{(2)} = \frac{\mathcal{Z}_{A_{i+1}}^{(2)}}{\mathcal{Z}_{A_i}^{(2)}}, \quad (10)$$

where A_i is a sequence of N blocks of increasing size such that $A_0 = \emptyset$ and $A_N = A$. Each of the ratios $R_{A_i, A_{i+1}}^{(2)}$ can be estimated efficiently, as it represents the ratio between the partition functions of systems which are 2β -periodic on regions A_i and A_{i+1} chosen so as to differ only by a few sites (or by a few interparticle spacings in continuum space). The Rényi entropy is then the sum of contributions from the successive increments ΔA_i that lead from \emptyset to A , $S_A^{(2)} = \sum S_{A_i, A_{i+1}}^{(2)}$ where $S_{A_i, A_{i+1}}^{(2)} = -\ln R_{A_i, A_{i+1}}^{(2)}$. While too large increments ΔA_i give rise to inefficient estimates of the corresponding ratios $R_{A_i, A_{i+1}}^{(2)}$, too small ones lead to a sizable accumulated error on the sum; yet an optimal size of the increment can be found minimizing the final error on $S_A^{(2)}$. In Fig. 2(a) we have used linear increments of size $\Delta A_i = \Delta l = 5$.

Nonetheless it can still be seen that the precision of the results is not optimal for $l_A \gtrsim 20$. This is a result of the slow increase of entanglement entropy in 1D systems (especially for $l_A \approx L/2$): if the ratios $R^{(2)}$ are known with a given relative error $\epsilon_R = \Delta R^{(2)}/R^{(2)}$, the corresponding entanglement increment $S^{(2)}$ has a relative error $\epsilon_S = \epsilon_R/S^{(2)}$, which can be much bigger than ϵ_R when the increment is small. This means that the QMC technique enjoys a faster scaling of the entropy, as found, e.g., in 2D systems or at finite temperature; as we will see, the quality of the 2D data is significantly better.

Having validated the approach against exact results, we can apply it to yet unexplored models. To demonstrate the versatility of the QMC Rényi entropy estimator, we apply it to the study of a model with continuous quantum variables, namely the 1D $O(2)$ quantum rotor model,

$$\mathcal{H} = -2J \sum_{\langle ij \rangle} \cos(\phi_i - \phi_j) - \frac{U}{2} \sum_i \frac{\partial^2}{\partial \phi_i^2}, \quad (11)$$

in which $\phi_i \in [0, 2\pi]$. This model represents an approximation to the Bose-Hubbard model with hopping J and repulsion U for large integer filling, and it exhibits a superfluid-insulator quantum phase transition for increasing U/J . Such a model can be studied via PIMC¹⁴ with discretized imaginary time (in steps $\Delta \tau$). Figure 2(b) shows the Rényi entropy for a chain of $L = 64$ sites at variable U/J ; we observe that for sufficiently small U/J the Rényi entropy obeys the CFT prediction

$$S_A^{(2)} = (\bar{c}/4)\ln[C(l_A|L)] + s_1, \quad (12)$$

where $\bar{c} = 1$, $C(x|L) = L/\pi \sin(\pi x/L)$, and $s_1 = s_1(U/J)$ is a constant dependent on the Hamiltonian parameters. On the other hand for large U/J the CFT prediction is no longer verified, as the system enters an insulating gapped phase.

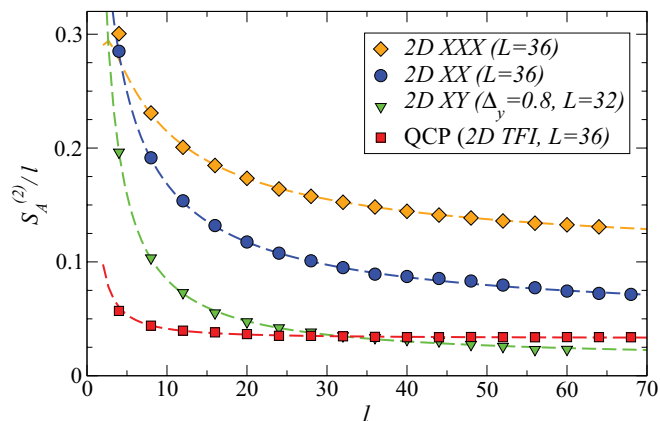


FIG. 3. (Color online) Entanglement entropy of 2D spin models with various symmetries; the error bars are smaller than the symbol sizes. The dashed lines represent fits to the form $b + c(\ln l)/l + d/l$.

IV. RESULTS FOR TWO-DIMENSIONAL MODELS

A. Effect of Hamiltonian symmetry

We then move to 2D systems, and consider three representatives of the three symmetry sectors of the XYZ model, Eq. (8) in zero field, namely the case of a $SU(2)$ invariant Heisenberg (or XXX) model ($\Delta_y = \Delta_z = 1$), the case of a $U(1)$ symmetric XX model ($\Delta_y = 1, \Delta_z = 0$), and the case of the Z_2 symmetric anisotropic XY model ($\Delta_y = 0.8, \Delta_z = 0$). In all three cases we consider A regions with a square geometry $l_A \times l_A$, grown in linear increments of (typically) five sites, and we plot the data as a function of the region boundary $l = 4(l_A - 1)$. The simulations have been performed with the SSE algorithm on lattices with $L \times L$ size up to $L = 36$, and at a temperature $\beta J \approx L$ guaranteeing the removal of thermal contributions.

The case of the XXX model has been previously investigated in Refs. 4 and 15 via projector QMC, and we confirm their finding of an area law scaling of entanglement entropy. As clearly shown in Fig. 3, an area law is also observed for the other two models with reduced symmetry: in all three cases the scaling of the Rényi entropy is very well fitted by an area law plus subleading corrections,

$$f(l) = bl + c \ln l + d; \quad (13)$$

the fit coefficients (obtained by discarding data with $l < l_{\min}$) are reported in Table I (see Appendix B for a discussion of the fits). In particular, the coefficient b of the dominant area-law term decreases systematically as the symmetry of the model is decreased; this is consistent with the picture that a lower symmetry confines quantum fluctuations to a restricted region of spin space, thereby lowering entanglement properties.

TABLE I. Fit coefficients for the three models investigated in Fig. 3.

Model	b	c	d	l_{\min}
2D XXX ($\Delta_y = \Delta_z = 1$)	0.099(1)	0.48(4)	0.05(10)	16
2D XX ($\Delta_y = 1, \Delta_z = 0$)	0.045(1)	0.31(3)	0.52(5)	8
2D XY ($\Delta_y = 0.8, \Delta_z = 0$)	0.013(1)	-0.02(2)	0.76(2)	8
2D TFI ($\Delta_y = \Delta_z = 0$)-QCP	0.0332(4)	-0.03(1)	0.15(2)	8

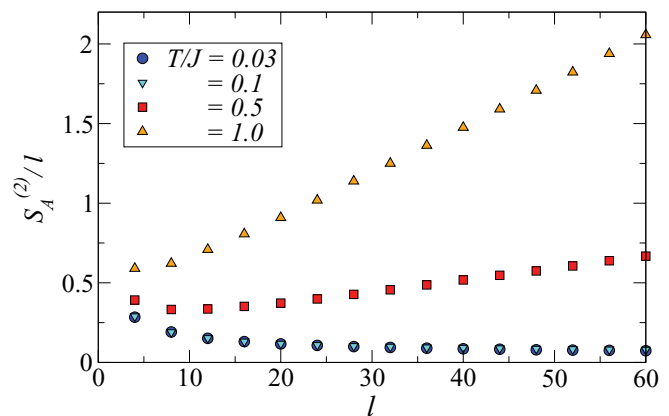


FIG. 4. (Color online) Rényi entropy for the 2D XX model at increasing temperature. Error bars are smaller than the symbol size.

B. 2D XX model and finite temperatures

The 2D XX model maps onto hard-core bosons, and it is directly relevant, e.g., to current cold-atom experiments. To make contact with a more realistic experimental situation, we have studied the effect of an increasing temperature on the scaling of the Rényi entropy, an aspect which can be quite naturally investigated with finite- T QMC. Given that thermal entropies are extensive, on general grounds one expects finite temperatures to introduce a *volume* law in the scaling, namely a $a(T)l_A^D$ term fatally masking the area-law term. Nonetheless the growth of the volume-law coefficient with temperature, $a(T)$, appears fairly slow: as shown in Fig. 4 an area law persists at a moderate, finite temperature, $T/J = 0.1$, for the block sizes considered here (the biggest being $l_A = 16$), implying that $a(T)l_A^D \ll 4b(l_A - 1)$. On the other hand, at a temperature $T/J = 0.5$ and higher, the volume law term dominates already for small block sizes. These results point to the fact that area laws of Rényi entropy are observable even at finite temperature and for moderate block sizes, which are indeed relevant for experiments.

C. Transverse-field Ising model at the quantum critical point

We conclude our discussion of $D = 2$ models with the case of the 2D transverse-field Ising (TFI) model, $\Delta_y = \Delta_z = 0$, which displays a quantum critical point (QCP) at $H_c \approx 1.52J$.^{16,17} Our approach enables us to investigate this two-dimensional quantum critical system in search of special entanglement signatures. As shown in Fig. 3 and in Table I, we observe that the entanglement Rényi entropy obeys an area law with a negative logarithmic correction and a positive additive constant. These findings are in quantitative agreement with recent field-theory results for a QCP with dynamical critical exponent $z = 1$, predicting universal negative logarithmic corrections coming from corners of the A region^{18,19} (see Appendix B), and a universal (α -dependent) additive constant in $D = 2$.²⁰ This shows that QMC simulations can quantitatively extract the subleading corrections; their universality can be directly tested by investigating different microscopic models exhibiting QCPs in the same universality class.

V. CONCLUSIONS

In this paper we have demonstrated a simple approach to incorporate an estimator of subsystem Rényi entropies into any finite-temperature quantum Monte Carlo scheme. This approach complements the estimator developed within the projector-QMC scheme,⁴ and it paves the way for a systematic investigation of entanglement entropies in a large variety of interacting quantum systems in arbitrary dimensions, such as quantum fluids, quantum spin systems, $O(N)$ quantum rotor models, quantum field theories, etc., as long as they are accessible to a QMC study. Contrary to DMRG or to variational methods based on tensor-network states, QMC simulations are completely unbiased with respect to the scaling of entanglement, and the QMC entanglement estimator actually performs better the faster the entanglement grows with the subsystem size. Moreover, QMC represents a natural platform to investigate the statistics of local quantum fluctuations in realistic systems, in the attempt to relate measurable fluctuation properties with entanglement properties.²¹

ACKNOWLEDGMENTS

T.R. acknowledges fruitful discussions with J. I. Cirac and R. Melko which sparked the present study. Both authors thank L. Tagliacozzo for discussions and a careful reading of the manuscript. All calculations have been performed on the computer cluster at the PSMN (ENS Lyon), whose support we gratefully acknowledge.

APPENDIX A: COMPARISON TO PREVIOUS METHODS

A few alternative methods have been recently proposed to extract the Rényi entropy of a subsystem via finite-temperature quantum Monte Carlo simulations. Here we discuss them critically, showing that they all present significant limitations compared to our approach.

1. Temperature-integration method

The most developed method is the one reported in Ref. 6, where the finite-temperature Rényi entropy of a region A is extracted via the following formula:

$$S_A^{(2)}(T) = \int_T^\infty \frac{dT'}{T'^2} \langle E \rangle_{A,T'} - \int_T^\infty \frac{dT'}{T'^2} \langle E \rangle_{\emptyset,T'} + 2S(T = \infty) + N_A \ln(D_H). \quad (\text{A1})$$

Here $\langle \dots \rangle_{A,T}$ denotes an average in the modified $\mathcal{Z}_A^{(2)}$ ensemble at temperature T , while $\langle \dots \rangle_{\emptyset,T}$ denotes an average in the \mathcal{Z}^2 ensemble of two disconnected replicas, and E is the energy estimator; N_A is the number of sites in the A region, and D_H is the dimension of the local Hilbert space on every lattice site. It is immediately evident that the last term in the above formula requires to work with a lattice system with $D_H < \infty$, excluding therefore continuous-space quantum field theories or lattice quantum field theories with an infinite-dimensional local Hilbert space (such as the quantum rotor model investigated in the main text). Moreover, the method of Ref. 6 consists in calculating separately the two integrals by numerical reconstruction of the energy estimators over a fine grid of temperatures. In general $\langle E \rangle_{A,T}$ and $\langle E \rangle_{\emptyset,T}$ tend to negative constants as $T \rightarrow 0$. Therefore each

of the integrals in Eq. (A1) *diverge* as T^{-1} when $T \rightarrow 0$; to extract the information on the entanglement ($T = 0$) Rényi entropy one needs *a priori* to reconstruct numerically the difference between two diverging quantities, which is subject to uncontrolled error, and which is in our opinion the limiting factor that prevented Refs. 6 and 7 from accessing the calculation of entanglement entropies on sizable systems.

In practice, to calculate the entanglement entropy in a system with a gapped spectrum it suffices to reach temperature $k_B T \approx k \Delta$, where Δ is the gap and $k \ll 1$. Hence the integrals in Eq. (A1) scale as $(k \Delta)^{-1}$. Moreover, the integrals scale as the system size L^D , given that the integrand is extensive. Therefore the error on the integrals scale as $(k \Delta)^{-1} L^D$ or as $(k \Delta)^{-1} L^{D/2}$ if self-averaging applies to the energy estimator (this is not the case, e.g., at quantum critical points and for systems with an extended critical phase at finite temperature, such as two-dimensional bosons or quantum spins with an easy-plane anisotropy). On the other hand, assuming that the linear size of the A region is proportional to the system size $l_A \sim L$, the entanglement entropy $S_A^{(2)}$ is expected to satisfy an area law (up to logarithmic corrections), and hence to scale as $S_A^{(2)} \sim L^{D-1}$. Therefore the relative error on $S_A^{(2)}$ scales as $(k \Delta)^{-1} L [(k \Delta)^{-1} L^{1-D/2}]$ if self-averaging applies to the energy]. If the system is gapless in the thermodynamic limit, the finite-size gap Δ vanishes as L^{-z} , and therefore the scaling of the relative error is $L^{1+z} (L^{1+z-D/2})$ with self-averaging of the energy). Therefore, the relative error becomes exceedingly big as L grows, even in the presence of self-averaging of the energy (e.g., if $z = 1$, one needs an unphysical $D > 4$ for self-averaging to apply to $S_A^{(2)}$).

This unfavorable scaling of the relative error on the entanglement Rényi entropy is in stark contrast with the scaling exhibited by our method. Our method reconstructs the entanglement Rényi entropy of a region of size $\sim L^D$ by the addition of $\sim L^D$ increments. The error on the sum of increments hence scales as $L^{D/2}$ (making use of a generalized central limit theorem which applies when L is sufficiently large, and which is verified by the consistency between our error bars and the scatter of our results). Hence the relative error for an entanglement Rényi entropy satisfying the area law scales as $L^{1-D/2}$, which means that we have no scaling for $D = 2$ and self-averaging for $D = 3$. Therefore, we find that our method offers a crucial inversion in the scaling of the relative error with the system size with respect to Ref. 6, allowing us to access efficiently the calculation of entanglement Rényi entropies in large systems.

2. Weight-ratio method and mixed-ensemble method

As mentioned in the main text, if the support of the \mathcal{Z}^2 ensemble and of the $\mathcal{Z}_A^{(2)}$ ensemble coincide, the partition function ratio $R_A^{(2)}$ giving the Rényi entropy can in principle be estimated directly by calculating the weight-ratio average $\langle w_A(\mathcal{C})/w_{A=\emptyset}(\mathcal{C}) \rangle_{\mathcal{Z}^2}$ within the \mathcal{Z}^2 ensemble. Here $w_A(\mathcal{C})$ is the weight of a configuration \mathcal{C} in the $\mathcal{Z}_A^{(2)}$ ensemble and $w_{A=\emptyset}(\mathcal{C})$ is the weight of the same configuration in the \mathcal{Z}^2 ensemble; both weights are nonvanishing if the support of the two ensembles is the same. This property is verified in quantum spin systems and lattice gases without conserved quantities, in

lattice systems with continuous local variables, and for models in continuous space. The above approach is applied, e.g., in Refs. 22–24 to Ising models and Ashkin-Teller models in $D + 1$ dimensions. We have implemented this approach for the case of the 1D quantum rotor model, and we find that this method is very inefficient for sufficiently large A regions. In what follows we outline the limitations of the approach.

If the A region is sufficiently big the two ensembles differ significantly, and hence the above weight-ratio estimator for $R_A^{(2)}$ corresponds to sampling the $\mathcal{Z}_A^{(2)}$ ensemble using the “wrong” weights of the \mathcal{Z}^2 ensemble. The $R_A^{(2)}$ estimator takes significant contributions only from rare \mathcal{C} configurations in the \mathcal{Z}^2 ensemble which have on the contrary a large weight in the $\mathcal{Z}_A^{(2)}$ ensemble, producing a large $w_A(\mathcal{C})/w_{A=\emptyset}(\mathcal{C})$ ratio. Hence the Monte Carlo time series of the $R_A^{(2)}$ estimator is composed of rare spikes, separated by long intervals in which the estimator is extremely small; this is a rather undesirable behavior for an estimator, implying very long autocorrelation times and slow convergence.

At a more quantitative level, we can set $w_A(\mathcal{C}) \sim \exp[-\beta S_A(\mathcal{C})]$, where $S_A(\mathcal{C})$ is the effective Euclidean action for the configuration \mathcal{C} and β is the inverse temperature. Given that the two ensembles $\mathcal{Z}_A^{(2)}$ and \mathcal{Z}^2 differ in the form of the effective action in the A region, we have that $S_A(\mathcal{C}) - S_{A=\emptyset}(\mathcal{C}) \approx a_c l_A^D$, and therefore $w_A(\mathcal{C})/w_{A=\emptyset}(\mathcal{C}) \sim \exp(-\beta a_c l_A^D)$, namely either exponentially small ($a_c > 0$) or exponentially big ($a_c < 0$) in the size of region A and in the inverse temperature. If the entanglement entropy satisfies the area law, the $R_A^{(2)}$ estimator must have an average of order $\exp(-\tilde{b} l_A^{D-1})$, namely exponentially small in the A region boundary and not in its volume. This mismatch has a strong consequence: the only way that the weight-ratio estimator can produce such an average is by exponentially (in βl_A^D) rare contributions with $a_c < 0$, separated by exponentially long waiting times giving exponentially small contributions (configurations with $a_c > 0$). To beat this autocorrelation effect, the simulation time should scale as $\exp(\beta l_A^D)$. This is to be compared with the estimated scaling as $(R_A^{(2)})^{-1} \sim \exp(\tilde{b} l_A^{D-1})$ of our method (see main text), involving the boundary of region A and not its volume, and independent of the inverse temperature. Therefore our approach offers an exponential speedup with respect to the weight-ratio method of Refs. 22–24. In principle, in the latter method one can use the same configuration \mathcal{C} for calculating the weight ratio for all possible translations of the A region in real space (if the system is translationally invariant) or in imaginary time; moreover, provided that one saves all the configurations of a simulation in the \mathcal{Z} ensemble in memory (which is impractical for a very long simulation), one can use any pair of such configurations to obtain one configuration in the \mathcal{Z}^2 ensemble.²² These two tricks provide a speedup which is only polynomial in β and in $l_A^D \sim L^D$, and therefore they cannot cure the exponential slowdown discussed above. The exponential scaling in the volume of region A can be alleviated by using the increment trick described in the main text.

Under the condition of same support for the \mathcal{Z}^2 ensemble and the $\mathcal{Z}_A^{(2)}$ ensemble, a further alternative method for the calculation of the Rényi entropy is proposed in Ref. 25. There

the Rényi entropy is calculated directly as

$$S_A^{(2)} = \beta \int_0^1 d\alpha \langle \mathcal{S}_{A=\emptyset} - \mathcal{S}_A \rangle_\alpha, \quad (\text{A2})$$

where the α ensemble, over which the average $\langle \dots \rangle_\alpha$ is taken, assigns to a configuration \mathcal{C} an action $(1 - \alpha)\mathcal{S}_A(\mathcal{C}) - \alpha\mathcal{S}_{A=\emptyset}(\mathcal{C})$. Therefore in practice the simulation is run in a “mixed” ensemble with effective long-range interactions in the imaginary-time direction. Similarly to the temperature-integration approach, this scheme has the inconvenient aspect that the entanglement entropy, which scales typically as the boundary of the A region, is expressed as the difference of two quantities scaling with the volume of the same region (assuming $l_A \sim L$ the scaling is with the volume of the whole system). Moreover, each term in the difference diverges as T^{-1} for $T \rightarrow 0$. A similar discussion as the one in the previous section applies.

APPENDIX B: ADDITIVE CORRECTIONS TO THE AREA LAW IN 2D QUANTUM SPIN SYSTEMS

Here we provide a more detailed discussion of the coefficients of the Rényi entropy scaling of a square subsystem embedded in a 2D quantum spin system. We fit our QMC data for 2D quantum spin models to the form $f(l) = bl + c \ln l + d$. On a $L \times L$ lattice, the fits are performed over a region of boundary sizes $[l_{\min}, 4(L/2 - 1)]$ whose lower bound l_{\min} is gradually increased to check convergence. Figure 5 shows the fit coefficients as a function of l_{\min} . As a general criterion, if convergence of the fitting parameters within the error bar is achieved for a given l_{\min}^* , we choose as best-fit parameters (shown in Table I of the main text) the ones corresponding to $l_{\min}^* - 4$ (given that they are consistent with the l_{\min}^* values and have smaller error bars). In general we observe that the coefficient of the area law b is very stable to variations of l_{\min} , while shrinking too much the fitting region leads to a transition in the coefficients of the subleading terms c and d . Nonetheless

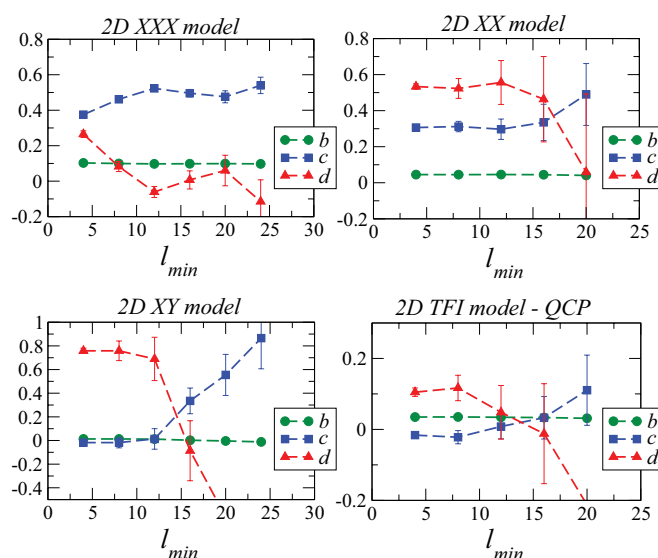


FIG. 5. (Color online) Evolution of the fit coefficients of $S_A^{(2)}$ when increasing the lower bound of the fit region $[l_{\min}, 4(L/2 - 1)]$.

we observe that convergence in the fitting coefficients is achieved before the transition; we observe that the transitions are systematically accompanied by a degradation in the precision of the resulting fit coefficients, and we argue that they can be attributed to the limited data sets that are left to fit if l_{\min} becomes too big. Such limited data sets mainly provide a reliable estimate for the coefficient of the leading term, but much less accurate estimates for the subleading ones. In particular, due to the degradation of the precision in the estimate of the subleading terms with the shrinking of the fitting region, it is not obvious *a priori* that one can capture correctly the asymptotic value of such terms—see below for further discussion.

Recent field-theoretical studies^{18,20,26,27} have pointed out that several two-dimensional quantum systems should exhibit a dominant area-law scaling of the entanglement entropy with a nonuniversal coefficient b —given that such coefficient would depend on the short-distance cutoff related to the details of the microscopic model of origin. On the other hand, the subleading logarithmic and constant terms can indeed be cutoff independent and universal. In the case of $z = 1$ quantum critical points (QCPs),²⁰ if the A region has a smooth boundary one expects that $c = 0$ and an additive universal constant d , dependent on the index α of the considered Rényi entropy. Our finding for the QCP of the 2D transverse field Ising (TFI) model is that d is indeed finite and positive for $\alpha = 2$; in the case $\alpha = 1$ (von Neumann entropy) Ref. 17 estimates as well a positive additive constant. On the other hand, we also find a finite logarithmic correction with a negative coefficient, $c = -0.03(1)$. One can relate this correction to contributions coming from corners of the boundary. Such a contribution to the c coefficient has been estimated in Ref. 18 for a free relativistic theory to be ≈ -0.0062 for each corner. Assuming that the linearly dispersing modes at the QCP in the 2D TFI model are described by such a theory, we obtain a value of c for four corners in quantitative agreement with our results. Nonetheless the appropriate field theory for the QCP is rather the interacting $O(1)$ model, and corner corrections might differ for that system, as pointed out in Ref. 19.

If the ground state has a finite correlation length (as is the case for the 2D anisotropic XY model), one expects a correlation-length-dependent additive constant d ;²⁰ the existing predictions of logarithmic corrections do not apply to this case. Indeed we find a sizable additive constant, and a

logarithmic correction which is consistent with zero. Finally, in the case of the 2D XX and XXX model, the ground state has an infinite correlation length and it develops long-range order in the thermodynamic limit. For the case of the 2D XXX model, fits to projector QMC data have been performed in Ref. 15 using the function $f'(l_A) = 4b'l_A + c'\ln(4l_A) + d'$ of the boundary size estimated as $4l_A$ (this estimate double-counts the corner spins). When fitted to the f' function our data deliver coefficients which are indeed in agreement with the ones quoted in Ref. 15.

Both the XX and the XXX model have linearly dispersing gapless Goldstone modes (two for the XXX model, and one for the XX model), each described in the long-wavelength limit by a free relativistic theory. Following Ref. 18 one could expect negative logarithmic corrections coming from corners, but in fact our results point towards a positive c coefficient for both models. This result is consistent with what was initially found numerically in Ref. 15, where positive logarithmic corrections have been shown to exist for the XXX model even in the absence of corners. Prompted by the results of Ref. 15, Ref. 27 has recently predicted that in systems exhibiting spontaneous symmetry breaking in the thermodynamic limit, one should expect a positive logarithmic correction with a coefficient c which takes the simple form $N_G(D - 1)/2$ where N_G is the number of Goldstone modes. This would imply that $c = 1$ for the 2D XXX model and $c = 1/2$ for the 2D XX model. Our observation is not consistent with this prediction, even when taking into account possible further negative logarithmic contributions coming from corners. Nonetheless we observe that the coefficient of the XXX model is significantly larger than that for the XX model. One might argue that a possible source of discrepancy between our results and those of Ref. 27 stems from the finite-temperature nature of our data. Indeed a temperature $T \sim L^{-1}$ (at which our simulations are conducted) is sufficiently low to eliminate Goldstone-mode excitations, but not to eliminate the thermal occupation of the low-lying tower-of-states excitations²⁸ (to eliminate those states one would need a prohibitively low temperature, $T \sim L^{-2}$); yet Ref. 27 suggests that in the case $L^{-2} \ll T \ll L^{-1}$ their prediction should still hold. A further source of discrepancy could be the fact that our finite-size results fail to correctly capture the behavior of the subleading terms in the limit $l \rightarrow \infty$. Future larger-scale simulations should be able to clarify this issue.

¹A. Rényi, *Proceedings of the Fourth Berkeley Symposium on Mathematical Statistics and Probability 1960*, edited by J. Neyman (University of California Press, Berkeley, 1961), p. 547 [http://digitalassets.lib.berkeley.edu/math/ucb/text/math_s4_v1_article-27.pdf].

²I. Peschel, *J. Phys. A* **36**, L205 (2003).

³J. Eisert, M. Cramer, and M. B. Plenio, *Rev. Mod. Phys.* **82**, 277 (2010).

⁴M. B. Hastings, I. González, A. B. Kallin, and R. G. Melko, *Phys. Rev. Lett.* **104**, 157201 (2010).

⁵P. Calabrese and J. Cardy, *J. Stat. Mech.* (2004) P06002.

⁶R. G. Melko, A. B. Kallin, and M. B. Hastings, *Phys. Rev. B* **82**, 100409 (2010).

⁷S. V. Isakov, M. B. Hastings, and R. G. Melko, *Nat. Phys.* **7**, 772 (2011).

⁸R. R. P. Singh, M. B. Hastings, A. B. Kallin, and R. G. Melko, *Phys. Rev. Lett.* **106**, 135701 (2011).

⁹D. M. Ceperley, *Rev. Mod. Phys.* **67**, 279 (1995).

¹⁰O. F. Syljuåsen and A. W. Sandvik, *Phys. Rev. E* **66**, 046701 (2002).

¹¹M. Boninsegni, N. V. Prokof'ev, and B. V. Svistunov, *Phys. Rev. E* **74**, 036701 (2006).

- ¹²References 22–24 exploit this aspect to estimate the entanglement entropy as $\langle w_A(C)/w_{A=\emptyset}(C) \rangle_{\mathcal{Z}^2}$ with a simulation in the \mathcal{Z}^2 ensemble. A further approach, based on a simulation in a “mixed” ensemble, is proposed in Ref. 25. See Appendix A for a detailed discussion.
- ¹³E. H. Lieb, T. D. Schultz, and D. C. Mattis, *Ann. Phys. (NY)* **16**, 407 (1961).
- ¹⁴M. Wallin, E. S. Sørensen, S. M. Girvin, and A. P. Young, *Phys. Rev. B* **49**, 12115 (1994).
- ¹⁵A. B. Kallin, M. B. Hastings, R. G. Melko, and R. R. P. Singh, *Phys. Rev. B* **84**, 165134 (2011).
- ¹⁶H. W. J. Blöte and Y. Deng, *Phys. Rev. E* **66**, 066110 (2002).
- ¹⁷A. previous calculation of the von Neumann entropy in the quantum critical 2D TFI model, based on a tensor-network algorithm, is reported in L. Tagliacozzo, G. Evenbly, and G. Vidal, *Phys. Rev. B* **80**, 235127 (2009).
- ¹⁸H. Casini and M. Huerta, *Nucl. Phys.* **764**, 183 (2007).
- ¹⁹R. R. P. Singh, R. G. Melko, and J. Oitmaa, *Phys. Rev. B* **86**, 075106 (2012).
- ²⁰M. A. Metlitski, C. A. Fuertes, and S. Sachdev, *Phys. Rev. B* **80**, 115122 (2009).
- ²¹H. F. Song, S. Rachel, C. Flindt, I. Klich, N. Laflorencie, and K. Le Hur, *Phys. Rev. B* **85**, 035409 (2012).
- ²²M. Caraglio and F. Gliozzi, *J. High Energy Phys.* 11 (2008) 076.
- ²³F. Gliozzi and L. Tagliacozzo, *J. Stat. Mech.* (2010) P01002.
- ²⁴V. Alba, L. Tagliacozzo, and P. Calabrese, *J. Stat. Mech.* (2011) P06012.
- ²⁵P. V. Buividovich and M. I. Polikarpov, *Nucl. Phys. B* **802**, 458 (2008).
- ²⁶H. Casini and M. Huerta, *J. Phys. A* **42**, 504007 (2009).
- ²⁷M. A. Metlitski and T. Grover, arXiv:1112.5166.
- ²⁸P. W. Anderson, *Basic Notions of Condensed Matter Physics* (Benjamin, Menlo Park, 1983), p. 45.